2007

Electromagnetic controlled cortical impact device for precise, graded experimental traumatic brain injury

David L. Brody
Washington University School of Medicine

Christine Mac Donald
Washington University School of Medicine

Chad C. Kessens
Washington University School of Medicine

Carla Yuede
Washington University School of Medicine

Maia Parsadanian
Washington University School of Medicine

See next page for additional authors

JOURNAL OF NEUROTRAUMA
Volume 24, Number 4, 2007

Pp. 657–673
DOI: 10.1089/neu.2006.0011

Electromagnetic Controlled Cortical Impact Device for Precise, Graded Experimental Traumatic Brain Injury

DAVID L. BRODY,[1] CHRISTINE MAC DONALD,[2] CHAD C. KESSENS,[3] CARLA YUEDE,[4] MAIA PARSADANIAN,[1] MIKE SPINNER,[1] EDDIE KIM,[1] KATHERINE E. SCHWETYE,[5] DAVID M. HOLTZMAN,[1,5,6] and PHILIP V. BAYLY[3]

ABSTRACT

Genetically modified mice represent useful tools for traumatic brain injury (TBI) research and attractive preclinical models for the development of novel therapeutics. Experimental methods that minimize the number of mice needed may increase the pace of discovery. With this in mind, we developed and characterized a prototype electromagnetic (EM) controlled cortical impact device along with refined surgical and behavioral testing techniques. By varying the depth of impact between 1.0 and 3.0 mm, we found that the EM device was capable of producing a broad range of injury severities. Histologically, 2.0-mm impact depth injuries produced by the EM device were similar to 1.0-mm impact depth injuries produced by a commercially available pneumatic device. Behaviorally, 2.0-, 2.5-, and 3.0-mm impacts impaired hidden platform and probe trial water maze performance, whereas 1.5-mm impacts did not. Rotorod and visible platform water maze deficits were also found following 2.5- and 3.0-mm impacts. No impairment of conditioned fear performance was detected. No differences were found between sexes of mice. Inter-operator reliability was very good. Behaviorally, we found that we could statistically distinguish between injury depths differing by 0.5 mm using 12 mice per group and between injury depths differing by 1.0 mm with 7–8 mice per group. Thus, the EM impactor and refined surgical and behavioral testing techniques may offer a reliable and convenient framework for preclinical TBI research involving mice.

Key words: behavior; controlled cortical impact; experimental traumatic brain injury; histology; mice

INTRODUCTION

TRAUMATIC BRAIN INJURY (TBI) is a major cause of death and disability, for which no effective treatment exists other than supportive care. A total of 5.3 million Americans—2% of the U.S. population—currently live with disabilities resulting from TBI (Thurman et al., 1999). Because many of the victims are young, the total costs to society in medical care and lost productivity are extremely high. However, despite substantial research effort, effective therapeutics have not been developed, and further preclinical and clinical research tools are needed (Narayan et al., 2002).

Animal models of TBI are critical in order to test mechanistic hypotheses and develop preclinical therapeutics (Lighthall et al., 1989; Meaney et al., 1994; Shohami et

Departments of [1]Neurology, [2]Biomedical Engineering, [3]Mechanical Engineering, [4]Psychiatry, [5]Anatomy and Neurobiology, [6]Molecular Biology & Pharmacology, Hope Center for Neurological Disorders, Washington University, St. Louis, Missouri.

al., 1995; Laurer and McIntosh, 1999; Duhaime et al., 2000; Bayir et al., 2003; Pineda et al., 2004; Faden et al., 2005; Kleindienst et al., 2005; Lenzlinger et al., 2005; Maegele et al., 2005; Maxwell et al., 2005; Prins et al., 2005; Thompson et al., 2005; Truettner et al., 2005; Buki and Povlishock, 2006; Marklund et al., 2006; Marmarou and Povlishock, 2006). There are many animal models of TBI, but only in transgenic mice can the effects of genetic factors be readily explored in an experimental setting. For example, the $\varepsilon 4$ allele of the apolipoprotein E gene (*APOE4*) may be a risk factor for poor outcome after TBI in humans (Jellinger, 2004), especially in younger patients (Teasdale et al., 2005). Several lines of transgenic mice expressing each of the ApoE alleles—E2, E3, and E4—have been produced (Xu et al., 1996; Sullivan et al., 1997; Sun et al., 1998), and initial studies indicate an ApoE allele-dependent effect on survival and cognitive outcome following experimental TBI in these animals (Sabo et al., 2000). TBI has been performed in mice with many other genetic manipulations, and these experiments have provided important insights (Longhi et al., 2001; Hartman et al., 2002; Uryu et al., 2002; Chang et al., 2003; Hlatky et al., 2003; Conte et al., 2004; Bayir et al., 2005; Abrahamson et al., 2006; Bermpohl et al., 2006; Kochanek et al., 2006).

In mice, the controlled cortical impact (CCI) model of experimental TBI is widely used because it yields consistent histological damage and behavioral deficits. Other techniques include weight-drop, impact acceleration, and fluid percussion models (Morales et al., 2005). In the CCI technique, mice are fully anesthetized, the skull is exposed, and a craniotomy is performed. Then, an impactor indents the exposed surface of the brain by a fixed distance at a fixed velocity. The mice recover well with minimal mortality, and have highly reproducible gross histological lesions in the underlying cortex and hippocampus. Importantly, they have consistent, moderately impaired performance on cognitive tasks such as the Morris water maze (Fujimoto et al., 2004; Saatman et al., 2006). CCI is generally performed using a pneumatic impact device that is supported by a solid metal frame. A milling table supporting the mouse and restraining apparatus can be used to precisely specify injury location relative to anatomical landmarks (Fox et al., 1998). Calibration and adjustment of gas pressures is performed to ensure reproducible impact velocities.

We have recently developed an electromagnetic impact device that attaches to an arm of a stereotaxic frame and delivers reproducible velocities without the need for frequent calibration. The device was capable of producing consistent, graded CCI injuries in adult mice with stereotaxic control of impact location and depth at high velocities. An earlier version of the device has been employed to produce closed skull impacts in a post-natal day 7 rat model at moderate velocities (Bayly et al., 2006).

METHODS

Device Design, Fabrication, and Calibration

During the initial design phase, the primary design goal was achievement of the desired velocity range while minimizing the size of the apparatus so that it could be used as a stereotaxic arm-mounted accessory. A wide variety of options were generated to this end. These options included the use of solenoids, CO_2 cartridges, pneumatics, spring and lever systems, and electromagnetic (EM) coils.

Of these, an EM coil-based design was chosen because it offered several advantages: (1) EM coil–based and solenoid-based designs appeared to be able to produce the highest velocities with the most compact devices. (2) In EM coil–based systems, a stationary magnet propels a wire coil, as opposed to a solenoid-based design in which a coiled wire generates a magnetic field that propels an iron core; this is advantageous because the coil is generally lighter than the iron core, making it easier to accelerate over short distances. (3) A coil can more easily be modified than a solenoid to allow for accessories such as sensors and alternative tip geometries. (4) Most importantly, the use of a true magnet makes the direction of the current through the coil significant; the direction of motion can be reversed simply by reversing the direction of the current through the coil, whereas in a solenoid-based design, a second element would be needed to reverse the direction of motion.

A moving coil design has one significant complication. When the coil moves in a magnetic field, a potential is created in the coil. The resulting voltage opposes the current through the coil, acting to decrease the velocity. Because this effect runs opposite the driving force, it is called a "back EMF," or backwards electro-motive force (EMF). The strength of this field is directly proportional to the speed of the motion, as given by the equation $V_B = k_t \nu$, where V_B is the back EMF, k_t is a proportionality constant dependent on the device, and ν is the velocity. Thus, the faster the coil moves, the stronger the opposing voltage becomes. The end result is that, at higher speeds, a higher voltage must be applied to the coil to induce currents.

We designed an EM coil-based impact device intended to be mounted on the arm of a stereotaxic instrument (Fig. 1A). A voice coil with stroke length 0.762 cm and coil mass 32.6 g (BEI Kimco, LA12-17-000A) was housed in a piston-like stationary cylinder (1.9 cm diameter) fab-

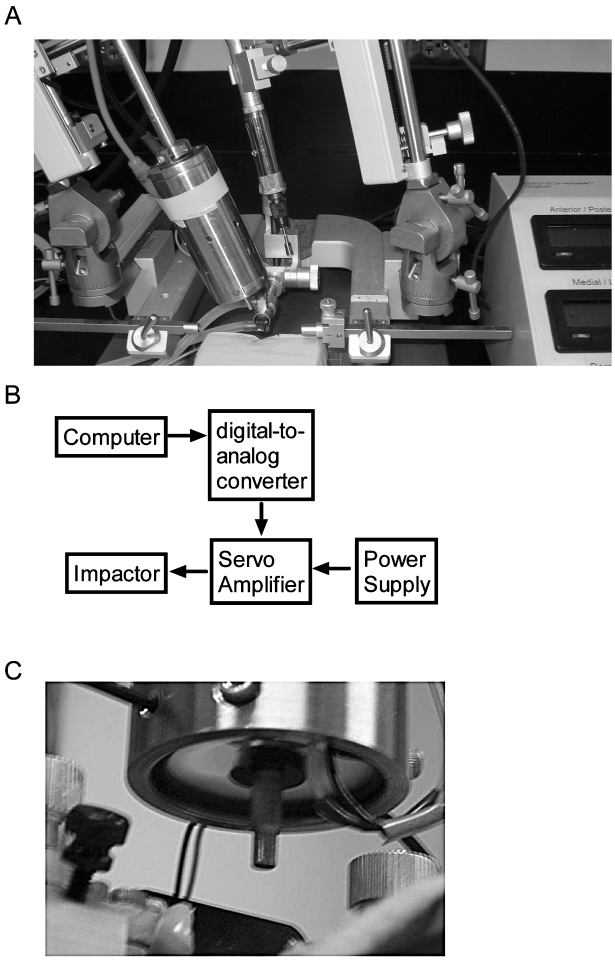

FIG. 1. Design of an electromagnetic controlled cortical impact device for experimental traumatic brain injury. (**A**) Photograph of the impactor device mounted on the left arm of a stereotaxic device. Motorized drill with 5-mm trephine mounted on the right arm. (**B**) Schematic of the components of the impact system. Control signals from a Windows-based notebook computer running custom Matlab™ routines are fed through a digital-to-analog converter. The digital-to-analog converter output is sent to a servo amplifier. The servo amplifier transmits current from 72-V power supply to the impactor containing an electromagnetic voice coil. This voice coil drives the impactor. (**C**) Photograph of the impactor tip in the raised position. A laser-Doppler displacement sensor was used to measure velocity of the tip during the impact stroke.

ricated to slip around the outside of the magnet and clamp around it. An inner ring of Delrin™ was added at the bottom of the cylinder as a stop; the semi-rigid ring distributes the stopping force and lessens deformation of the piston upon impact. A thin layer of padding was added to the magnet to cushion the coil's impact at the top of its up-stroke, significantly extending the life of the device. Air "vents" were milled into the sides of the piston to prevent any pressure differential which would reduce acceleration. The outer surface of the piston and the inner surface of the cylinder were polished to minimize friction between the two surfaces. The total mass of the device, the mass of the moving components, and the force generated were designed to be relatively small (no larger than necessary for mouse CCI), in order to avoid the necessity for the large, metal crossbar commonly used with pneumatic CCI devices.

To control the motion of the EM coil, several electronic devices were incorporated to provide the required current to the actuator (Fig. 1B). A servo amplifier (B12A8; Advanced Motion Controls, Camarillo, CA) provided approximately 1.75 amps/commanded volt. A 72-V power supply (PS300W; Advanced Motion Controls) was required in order to overcome the back EMF effect and achieve the desired velocities. A standard Windows laptop running Matlab™ (version 14; The Mathworks, Natick, MA) in combination with a NI-DAQ digital-to-analog converter (DAQCard 6062E; National Instruments, Austin, TX) was used to communicate control commands to the amplifier.

In the custom-written operating software, the user begins by entering a desired command voltage (or accepting a default voltage). Once the voltage is accepted, a small current is applied, ensuring that the impactor is fully extended in its downward position. The user is then prompted to position the impactor in the desired location. Once the "zero" position has been verified, a short, strong current pulse raises the impactor to its cocked position, and a lighter current maintains the position. The user is then prompted to lower the device to the desired impact depth. The depth of impact is thus specified using the controls intrinsic to the stereotaxic instrument. The user presses "Enter" to initiate impact. The current specified by the user at the start of the program is then delivered, causing an impact at the desired velocity, and the impactor is retracted after an adjustable dwell time, specified via the Matlab-based control software. For these experiments, the dwell time was typically 100 msec.

To calibrate the relationship between applied command voltage and tip impact velocity, the displacement of the impactor was measured with a fast, non-contacting laser displacement sensor (LD1605-10; Micro-Epsilon, Germany; Figs. 1C and 2). This displacement sensor acquired samples at a rate of 10,000 Hertz. Data was acquired using Matlab Version 14 in combination with NI-DAQ routines. Velocity was defined over the final 10% of the stroke range. Overshoot was defined as the maximum, transient displacement of the tip during the stroke beyond the user-specified set distance. For comparison, the relationship between applied pressure, tip impact velocity, and overshoot was also similarly de-

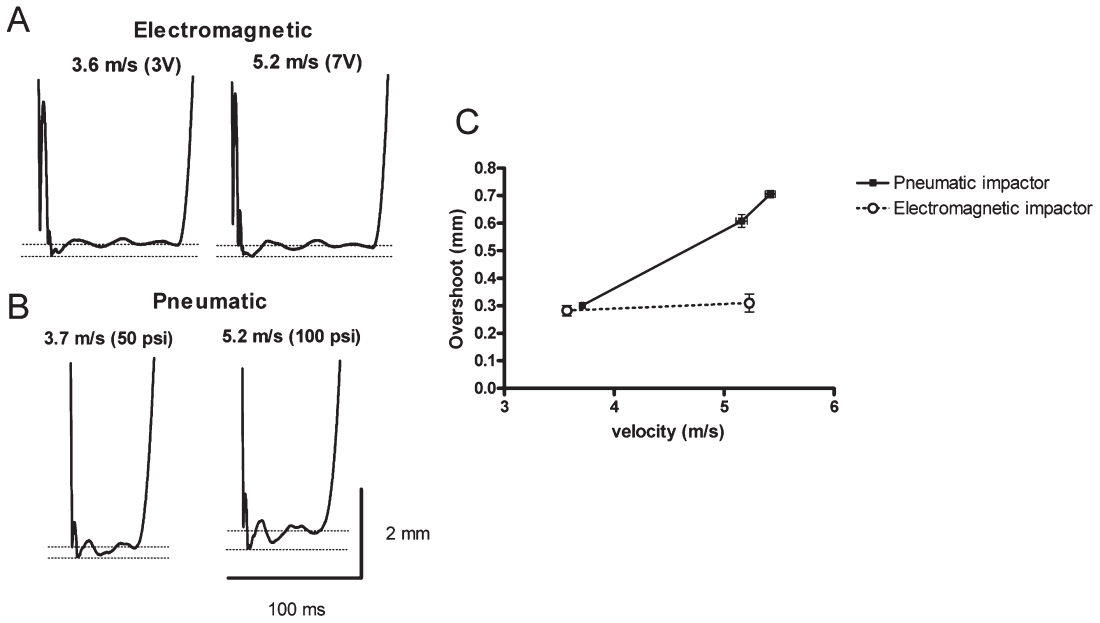

FIG. 2. Trajectories of the impactor tip during impact stroke: measurements of velocity and overshoot. All trajectories were measured using a fast laser Doppler displacement sensor aimed at the tip of the impactor. (**A**) EM impactor set at 3 or 7 V, yielding velocities of 3.6 or 5.2 m/sec. Overshoot, defined as the transient excursion of the impactor tip past the set distance specified by the user, was 0.31 ± 0.032 mm at 7 V and essentially unchanged at 3 V. Set distance and overshoot are indicated by top and bottom dashed lines, respectively. (**B**) Pneumatic impactor (Amscien, AMS201) with high-pressure settings of 50 or 100 psi yielding velocities of 3.7 or 5.2 m/sec. (**C**) Overshoot as a function of velocity for the electromagnetic and pneumatic impactors. Overshoot was strongly velocity-dependent for the pneumatic impactor as tested but there was little change in overshoot with velocity for the electromagnetic impactor.

termined for a commercially available pneumatic CCI device (Amscien, Richmond, VA).

Experimental Traumatic Brain Injury in Adult Mice

All experiments were approved by the animal studies committee at Washington University. Young adult B6SJLF1 wild-type mice (age 2–3 months) of both sexes were purchased from Jackson Labs (Bar Harbor, ME). The mice were housed in the Washington University animal facilities under standard conditions at 4–5 mice per cage. They were given standard lab chow and water *ad libitum*; cages were changed twice per week. They were maintained in a controlled temperature environment with lights on for 12 h and lights off for 12 h per day.

Mice were subjected to a single left lateral CCI with craniotomy (Dixon et al., 1991; Smith et al., 1995, 1998; Murai et al., 1998). Mice were anesthetized with isoflurane, 5% for induction and 1.5–2% for maintenance. They were placed in a stereotaxic frame with an incisor bar at 0° and cup head holders (David Kopf Instruments, Tujunga, California). The cup head holders were used to avoid the potential for injury to the ear canals produced by earbars in mice. Several lines of transgenic mice appear to be more susceptible to ear canal injury than wild-type mice and younger mice may also be more susceptible than older mice (D. Brody, unpublished data). The head holders were applied such that the most anterior portion of the cup was aligned with the posterior canthi of the eyes of the mouse. A consistent mild compression of the skull was applied by holding the head with the two cup head holders a consistent distance apart: 10.7 mm for female mice weighing 18–20 g and 11.7 mm for male mice weighing 24–26 g. These distances were assessed using the rulings on the bars (Kopf) that anchor the cup head holders to the frame. Rectal temperature was maintained at 37°C with a warming pad and feedback controller (Cell Microcontrols, Norfolk, VA). Ointment to protect vision was applied to their eyes, and their heads were shaved with an electric clipper. All tools were sterilized with a glass bead sterilizer. The skin was prepped with betadine ointment, and the top of the skull was exposed with a 1-cm skin incision.

A craniotomy was performed over the left parietotemporal cortex using a 5-mm trephine (Meisinger, Neuss, Germany) attached to an electric drill (Foredom, Bethel, CT) mounted on the right stereotaxic arm (Fig. 1A) of a

digital stereotaxic device (Benchmark Deluxe™; MyNeurolab, St. Louis, MO), though the device can be used with any compatible small animal stereotaxic system. The angle of the drill and the head of the mouse were adjusted so that the craniotomy penetrated the thin skull of the mouse without damaging the dura. There was a consistent, mild compression of the skull produced by the cup head holders, which caused the surface of the brain to protrude through the craniotomy. The maximal extent of this protrusion was approximately 0.4 mm, as measured using a fine probe attached to one arm of the stereotaxic device. In two of 80 mice, injury during the craniotomy resulted in swelling greater than 0.5 mm and/or bleeding from the dura. These two mice were disqualified and not used for any further experiments. The drill was then rotated out of the field, and the 5-mm disc of bone was removed using a 1-mm cup rongeur and spatula (Roboz, Gaithersburg, MD).

Next, the impact device mounted on the left stereotaxic arm at an angle of 15° from vertical was rotated into the field. The right edge of the 3-mm tip of the impact device was aligned with the midline suture and the posterior edge of the tip was aligned with the horizontal portion of the lambda suture using the stereotaxic arm. Because the EM cylinder was relatively bulky (37 mm diameter), visualization of the EM tip was somewhat more difficult than visualization of the pneumatic device tip (9.5-mm diameter). This minor disadvantage was compensated for by the use of a hand lens or operating microscope to confirm all alignments. The tip was positioned over the left fronto-parietal cortex by moving it 1.5 mm anteriorly and 1.2 mm to the left using the digital stereotaxic arm. This resulted in an impact centered 3.0 mm anterior to lambda and 2.7 mm left of midline, within the craniotomy. The zero depth position was determined by aligning the tip of the impact device in the down position with the surface of the dura. A low-voltage DC circuit touch detector (custom built by the Washington University Electronics Shop) was used to determine when the tip first contacted the dura. One electrode was clipped to the impactor tip and the mouse's hind paw was placed in contact with a second electrode. The surface of the dura was typically dry, but when fluid or blood was present, this was cleaned and dried carefully using irrigation with sterile saline and sterile, dry cotton swabs before the zero depth was determined. Contact was verified using a hand lens or operating microscope for every impact. The tip was raised to the cocked position, and the depth of desired impact was set by lowering the impact device 1–3 mm using the stereotaxic arm. Correction for overshoot was not made. CCI was triggered using Matlab-based computer controller. Velocities were controlled by setting the voltage command to the digital-to-analog converter. For most experiments, a 7-V command was used, corresponding to a 12.25-amp current pulse to the actuator, and resulting in a 5.23 $\pm$ 0.03 m/sec stroke velocity.

Bleeding of the injured cortical surface was controlled using copious irrigation with room-temperature sterile saline. The skull was dried, and a 6-mm-diameter plastic disc was glued with Vetbond to the skull to cover the craniotomy defect and prevent infection. These discs were produced by the Washington University Machine Shop from commercially available weigh-boats. The skin was closed with five to six interrupted sterile 4-0 nylon sutures. Triple antibiotic ointment was applied to the skin. Mice were removed from the stereotaxic frame and placed on a warming pad while they recovered from anesthesia. Sham-injured animals went through the same procedure but did not undergo CCI. The entire procedure required ~20 min per mouse.

In ~5% of mice, brief seizure activity was observed during emergence from anesthesia but this always ceased without intervention. The mice typically began to move spontaneously within 15 min. Mice were returned to their home cages when fully ambulatory, typically 30–120 min after injury. When mice appeared lethargic, they were housed singly for up to 48 h and then returned to their home cages. Mice were weighed at baseline and daily for 2 days. Those with weight loss greater than 30% were sacrificed. Those with weight loss of 20–30% were singly housed with food and water in the bottom of the cage. Wounds were inspected daily for 2 days and then weekly thereafter. Dehiscences were resutured under isoflurane anesthesia.

For CCI using a pneumatic device (Amscien, AMS 201), an identical procedure was used with the following modifications: (1) The 3-mm-diameter impactor tip was positioned relative to midline and lambda using a milling table inside the frame of the pneumatic impact device upon which the stereotaxic frame was placed (Fox et al., 1998). (2) The depth of injury was set using the screw-mounted adjustment provided as part of the pneumatic CCI device. (3) A dwell time of 50 msec was used. (4) A velocity of 5.16 $\pm$ 0.05 m/sec was obtained using settings of 100 pounds per square inch (psi) for the high pressure and 20 psi for the low pressure. A 54-inch cylinder of compressed nitrogen (Airgas, Inc., St. Louis, MO) connected via a regulator (Concoa model 3124391-01-580) drove the device. We found that smaller cylinders of compressed gasses, even when yielding nominally similar baseline pressures, were not able to drive the device with the desired velocities, even at maximal settings. This may be because of larger drops in pressure at the time the device discharges observed with the smaller tanks.

Behavioral Testing

Morris water maze. Morris water maze testing was performed starting 13 days following experimental TBI. Each mouse was given four trials per day for 3 days with a clearly visible platform and then 4 trials a day for 5 days with the platform in a different location hidden beneath the surface of the opacified water. Each trial lasted a maximum of 60 sec. The platform was 11 cm in diameter; the pool was 109 cm in diameter. A single, 30-sec probe trial was performed after the last day of hidden platform testing. In other respects, testing was identical to that previously described (Brody and Holtzman, 2006).

Rotorod. Rotorod testing was performed starting 24 days following TBI. In this test of motor learning, mice were placed on an accelerating, rotating, horizontal cylinder (Crawley, 2000). The amount of time that the mice are able to stay on the cylinder without falling off is often used as a measure of motor skill adaptation, as the mice must accelerate with the cylinder. Mice were tested with two 180-sec trials per day on each of 3 days. To control for gross motor impairments and any behavioral abnormalities that would interfere with interpretation of the results (such as jumping off of the platform voluntarily), mice were placed on the cylinder while it rotated at a constant, slow speed for two 60-sec trials each day. Prior to testing each day, mice were placed on the cylinder once for 60 sec while it was stationary to allow them to adapt to it.

Conditioned fear. Conditioned fear testing and shock sensitivity testing were performed starting 38 days after TBI (Crawley, 2000; Khuchua et al., 2003). In this test of associative, non-spatial memory, mice were first exposed to a 1.0-mA continuous brief foot shock associated with a cue; in our experiments, this was an 80-dB, 2800-Hz tone. The amount of time freezing was monitored as a measure of their fear response. The next day, the mice were placed in the same experimental chamber where the initial shock occurred, and again time spent freezing was assessed with no shock. This indicates how well they associated the environmental context with the shock. On the third day, the amount of time spent freezing in a novel context when they were exposed again to the cue was measured, as an indication of how well they associated the cue with the shock. This was performed in a different experimental chamber from the one used in the initial association. Shock sensitivity and time spent freezing at baseline were assessed in order to control for differences in freezing behavior between mice that were not related to associative memory.

Histological Analysis

A randomly selected subset of the mice were deeply anesthetized with isoflurane and sacrificed after behavioral testing was complete, or for animals not tested behaviorally, 30–45 days after TBI. Mice were perfused intracardially with ice-cold heparinized 0.9% saline. Brains were carefully removed, fixed in paraformaldehyde, and equilibrated in 30% sucrose (Holtzman et al., 2000). Every sixth 50-μm frozen section was mounted on glass slides (Fisher, Superfrost Plus) and stained with bis-benzamide or cresyl violet. For each section containing visible hippocampus (bregma -0.94 mm to -3.88 mm) (Franklin and Paxinos, 1997), four contours were traced, and their areas were measured using the Stereo Investigator Contour Tracing Tool (*Stereo Investigator Users Guide*, version 6, MicroBrightField, Inc.). The four contours were the ipsilateral and contralateral hippocampus, and ipsilateral and contralateral dorsal cortex. The inferior border of the dorsal cortex was defined by a horizontal line touching the bottom margin of the dorsal third ventricle. The sections analyzed contained both dorsal and ventral hippocampus. Volumes were estimated using the Cavalieri principle (Howard and Reed, 2005); the areas over the 9–10 sections traced for each mouse were summed and multiplied by the spacing between sections (300 μm). Thus, the volumes obtained represent the complete extent of the hippocampus, and the dorsal cortex in the region overlying the hippocampus.

Statistical Analysis

All data was analyzed using Statistica 6.0 (StatSoft, Tulsa, OK). Factorial analysis of variance (ANOVA) was used for all behavioral analyses; impact depth, mouse gender, and experimenter performing the injury were categorical predictor variables. The Tukey HSD test was used to determine post-hoc statistical significance of pairwise comparisons between groups. For visible and hidden platform Morris water maze data, repeated measures ANOVAs were used with performance averaged across each of the four daily trials, and day of training used as the repeated measure variable. For probe trial data, 95% confidence intervals were calculated and compared to performance expected by chance. For rotorod data, repeated measures ANOVAs were used with performance averaged across the two trials per day; and day of training used as the repeated measure variable. One-way ANOVAs were used for analysis of hippocampal and cortical volumes.

For statistical power calculations of sample size requirements, a Monte-Carlo approach was used. A custom-written Visual Basic macro running inside of Statistica generated 150 random sub-samples of the mice

subjected to either 2.0-mm or 3.0-mm injury. The hidden platform data for each of these sub-samples was then analyzed using repeated measures ANOVA. The probability that each mouse would be picked during the random sub-sampling was varied to produce sub-samples with varying sample sizes. The *p*-values were tabulated as a function of sample size, and the median and upper 80% confidence interval was calculated using Statistica. This allowed exploration of the sample size needed to achieve an 80% likelihood of detecting a statistically significant difference between groups with the characteristics of these two injury severities.

RESULTS

Device Mechanical Characteristics

The velocity and overshoot of the EM CCI impactor during its full stroke were compared with the trajectory of an Amscien AMS 201 pneumatic CCI device (Fig. 2). With the power supply of the EM device set at 7 V, the end impact velocity was 5.23 ± 0.026 m/sec, whereas with the power supply set at 3 V, the velocity was 3.57 ± 0.032 m/sec. No statistically significant differences were observed when the device was retested with the same voltage settings several weeks later without recalibration or adjustment of the device. At 5.2 m/sec, there was a small overshoot, 0.31 ± 0.032 mm. Stated another way, the maximum depth the tip of the impactor reached during its trajectory was 0.31 mm deeper than the depth set by the user. At 3.6 m/sec, there was little change in the overshoot, 0.28 ± 0.019 mm. In contrast, the pneumatic device tested produced a 0.61 ± 0.047 mm overshoot at 5.2 m/sec, and at 3.7 m/sec the overshoot was substantially reduced to 0.30 ± 0.016 mm. Thus, the overshoot was velocity-dependent in the pneumatic device tested but not in the prototype EM device, in the range of velocities tested. Overall, there was significantly greater overshoot in the pneumatic device tested than in the EM device at 5.2 m/sec but little difference between the devices at 3.6 to 3.7 m/sec.

We investigated whether the measured overshoot arises from mechanical deformation of the structural supporting elements holding the impactors, as opposed to dynamic compression of the materials used to stop the stroke of the pistons. For the EM impactor, we used the laser Doppler to record the movement of the distal end of the horizontal portion of the stereotaxic arm holding the impactor device during its full stroke. We found a maximum displacement of 0.336 ± 0.054 mm at 5.2 m/sec, which was statistically indistinguishable from the overshoot measured at the impactor tip (0.31 ± 0.032 mm). At 3.6 m/sec, the maximum displacement was 0.278 ± 0.013 mm, also indistinguishable from the tip overshoot (0.28 ± 0.019 mm). We therefore conclude that the overshoot of the tip of the EM device can be entirely explained by the mechanical deformation of the stereotaxic arm holding the impactor.

For the pneumatic impactor tested, we measured the movement of the bottom surface of the vertical metal guide supporting the pneumatic cylinder during the full stroke of the device. During a 5.2 m/sec stroke, the maximum displacement was 0.51 ± 0.11 mm, and during a 3.7 m/sec stroke the maximum displacement was 0.268 ± .004 mm. Similarly, the maximum displacement at the center of the large metal crossbar supporting the pneumatic cylinder, guide and alignment apparatus was 0.427 ± 0.01 mm at 5.2 m/sec and 0.29 ± 0.005 mm at 3.7 m/sec. The movement of the supporting structures appeared to largely explain the total overshoot measured at the tip.

Histological and Behavioral Characteristics of Injury

We performed single CCI injuries on fully anesthetized young adult B6SJLF1 mice with a range of impact depths from 1.0 to 3.0 mm in 0.5-mm increments. Most mice recovered well from the injury and were able to ambulate within 20 min of injury. Four mice that sustained 3.0-mm impacts were lethargic and lost 10–20% of their body weight for the first 1–2 days after injury. These mice were singly housed with food and water placed on the floor of the cage. In total, two of the 25 mice impacted at a depth of 3.0 mm died; the rest recovered, regained the weight that they had lost, and were returned to their home cages. No mice in the other groups had significant weight loss or died as a result of the experimental TBI. A total of two other mice died prior to injury: one due to temperature controller malfunction causing hyperthermia and one due to apnea during isoflurane anesthesia.

We assessed the histological effects of injuries produced by the EM CCI device at a velocity of 5.2 m/sec. There was no histological evidence of injury to cortex or hippocampus in mice in the sham group (Fig. 3). As the depth of the impact increased, there was a progressive loss of cortical and hippocampal tissue, and distortions in the morphology of the remaining hippocampus and cortex. Thinning of the hippocampal pyramidal cell layers was apparent (Fig. 3A). The extent of tissue preservation was assessed by an examiner blinded to the impact depth 1 month after the injury. As the depth of impact increased, there was a decrease in the fraction of spared tissue, as measured relative to the contralateral side (Fig. 3B). The effect of impact depth was highly significant for the fraction of spared tissue in hippocampus ($F_{4, 23} = 15.6$, $p <$

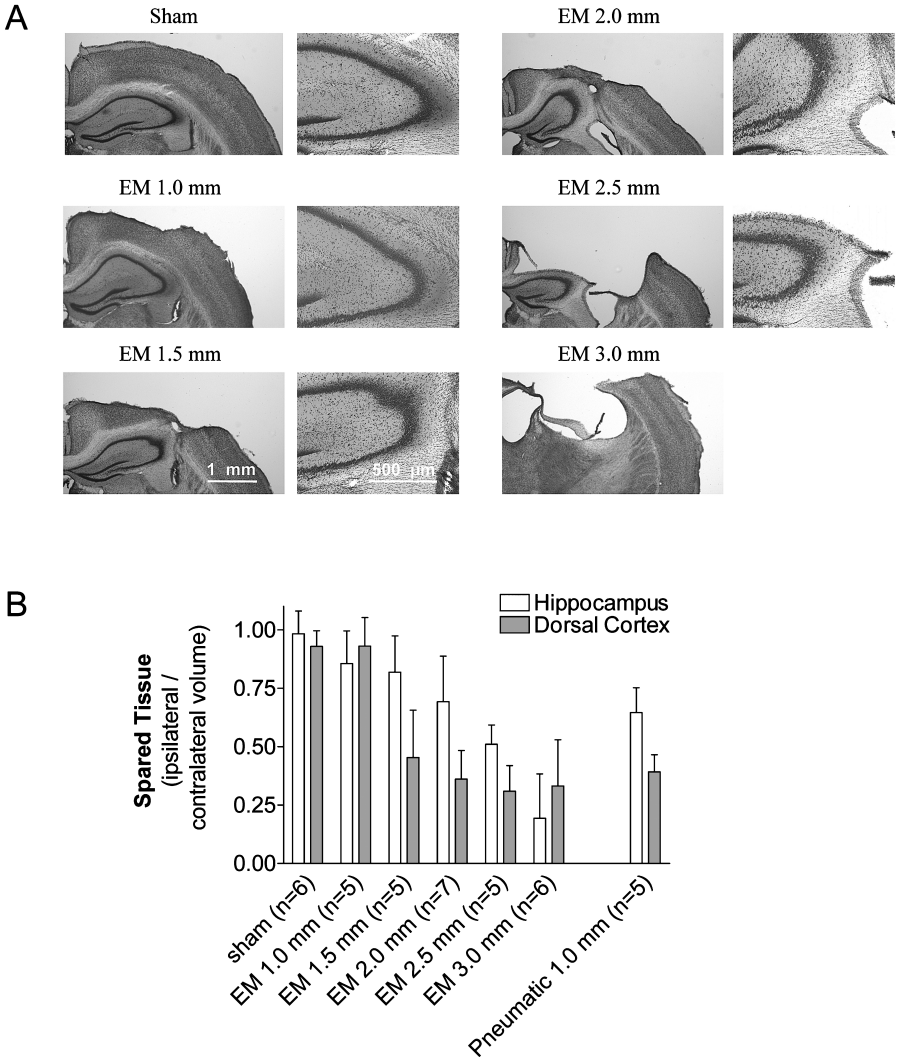

FIG. 3. Histological analysis of injuries produced by EM and pneumatic devices. (**A**) Histological images of cresyl violet–stained coronal sections following sham injury, and 1.0, 1.5, 2.0, 2.5, and 3.0 mm impact using the EM device. Left images in each pair show overall dorsal cortical and hippocampal tissue loss and architecture. Right image in each pair show further details of hippocampal architecture. Cortical and hippocampal tissue injury and anatomical distortion increase in a graded fashion with increased impact depth. All images were obtained from slices through the same anatomical region (bregma −1.7 mm), selected based on the architecture of the contralateral hemisphere. (**B**) Proportion of spared ipsilateral hippocampus and dorsal cortex remaining 1 month after TBI. Each stereologically determined hippocampal or cortical volume was normalized by the corresponding contralateral volume for that animal. Set depth of injury on the *x* axis. Error bars represent standard deviations. All injuries were performed by the same investigator and volumes were assessed without knowledge of device or impact set depth.

0.0001) and cortex ($F_{4,\ 23} = 14.3$, $p < 0.0001$). At 1.0-mm depth, there was minimal injury in either cortex or hippocampus. At 1.5-mm depth there was significant cortical injury and mild cell loss in the underlying hippocampus. At 2.0-mm and 2.5-mm depths, there was progressively more injury to the hippocampus and cortex. At 3.0-mm depths, the hippocampus was nearly destroyed. Mice injured at this depth also had thalamic lesions (not shown), which were not assessed in a quantitative fashion. The standard deviations represent injury variability and not measurement error, as intra-rater reliability testing revealed a ~3% error in volume measurements (not shown). There was no apparent injury to the contralateral hippocampus or cortex in any of the animals (not shown), although ultra-sensitive techniques, such as de Olmos silver staining, were not used (Hall et al., 2005b). This indicated that the EM CCI device can produce a broad range of CCI injuries in a reliable fashion.

For comparison, we produced pneumatic CCI injuries at a commonly used depth of 1 mm (Smith et al., 1995; Fox et al., 1998; Hall et al., 2005a) in mice of the same age and strain. This produced a moderately severe injury to cortex and hippocampus, as has been reported previously. This 1.0-mm depth impact with the pneumatic CCI device was most similar to the 2.0-mm impact produced by the EM CCI device. This discrepancy cannot entirely be explained by the difference in overshoot between the two devices.

Next, we performed behavioral testing on mice subjected to a range of injury severities. Again we found a graded effect of impact depth of behavioral impairment in Morris water maze (Fig. 4) and rotorod (Fig. 5) testing. For visible platform water maze performance, there were statistically significant effects of injury group (control vs. each of three impact depths. $F_{3, 41} = 9.95$, $p < 0.0001$) and test day ($F_{2, 82} = 166.2$, $p < 0.0001$; repeated-measures ANOVA). For hidden platform water maze performance, there were statistically significant effects of injury group ($F_{3, 41} = 18.0$, $p < 0.0001$), test day ($F_{4, 164} = 17.1$, $p < 0.0001$), and the interaction of injury group and test day ($F_{12, 164} = 2.99$, $p = 0.0008$). For water maze probe performance, there were statistically significant effects of injury group ($F_{3, 41} = 20.8$, $p < 0.0001$ for target quadrant and $F_{3, 41} = 10.0$, $p < 0.0001$ for exact target zone). For constant velocity rotorod performance, there were statistically significant effects of injury group ($F_{3, 43} = 9.9$, $p < 0.0001$) and test day ($F_{2, 86} = 32.7$, $p < 0.0001$). For accelerating rotorod performance, there were statistically significant effects of injury group ($F_{3, 43} = 11.7$, $p < 0.0001$) and test day ($F_{2, 86} = 33.3$, $p < 0.0001$). There were no significant differences between injured and sham mice in terms of conditioned fear performance. All mice performed well in this test with a 24-h interval between conditioning and testing, regardless of injury status.

Mice with 2.0-mm impacts were impaired in water maze performance relative to sham-injured controls but had normal rotorod performance. In visible platform testing (Fig. 4A; days 13–15), 2.0-mm-impacted mice had poorer performance than sham mice on the first day of testing, but both groups performed equally well by the third day of testing. This indicates that the 2.0-mm-impacted mice may have had some initial procedural impairment, but that their vision, swimming ability and motivation to escape from the pool was unimpaired overall. Hidden platform performance, however, was impaired (Fig. 4A; days 17–21) relative to sham mice ($p = 0.006$, repeated measures ANOVA followed by Tukey post-hoc test). Although impaired, 2.0-mm-impacted mice improved their performance over the 5 days of hidden platform training. Time and distance measures of performance showed equivalent results. Swim speed did not differ appreciably between groups (data not shown). The probe trial performance (Fig. 4B) of 2.0-mm-impacted mice was significantly better than chance in terms of time spent in the target quadrant. However, their performance was not above chance in terms of time spent in the exact region where the platform had been located. Instead, sham mice did perform better than chance in both measures. This suggests that 2.0-mm-impacted mice were capable of forming spatial memories, but that their spatial maps were less precise than those formed by sham mice. Rotorod performance was not significantly different between 2.0-mm-impacted mice and sham mice (Fig. 5).

Mice with 2.5-mm impacts were impaired in water maze and rotorod performance relative to both sham-injured controls and 2.0-mm-impacted mice. Visible platform performance (Fig. 4A; days 13–15) was worse compared to sham mice ($p = 0.039$), although they were able to find the platform in under 10 sec on average by the third day. Hidden platform performance (Fig. 4A; days 17–21) appeared more impaired in 2.5-mm-impacted mice than in 2.0-mm-impacted mice, though this did not reach statistical significance, and was profoundly impaired relative to sham mice ($p = 0.0002$). There was little learning over time, and in the probe trial (Fig. 4B), performance was at or below chance levels, indicating that these mice had not formed detectible spatial memories. Mice with 2.5-mm impacts were also impaired on the accelerating phase of the rotorod testing (Fig. 5C) relative to sham mice ($p = 0.016$). Their performance on the stationary and constant speed portions of the rotorod testing was normal. Overall, these results suggest that they had deficits in motor learning in addition to poor spatial learning.

Mice with 3.0-mm impacts were severely impaired in both water maze and rotorod performance. During visible platform water maze testing, two of 12 mice failed to reliably swim to the platform and were disqualified from further water maze testing. The visible platform performance of those that were not disqualified (Fig. 4A) was still markedly worse relative to sham mice ($p = 0.0002$) and relative to 2.5-mm-impacted mice ($p = 0.038$) or 2.0-mm-impacted mice ($p = 0.005$). This likely reflects a deficit not only in spatial learning and memory but also in learning procedural aspects of the test, such as swimming ability, vision, and motivation to escape from the water. Their hidden platform performance was significantly worse than 2.0-mm-impacted animals ($p = 0.005$) or sham mice ($p = 0.0002$). Floor effects may have prevented statistical resolution of further impairment relative to 2.5-mm-impacted mice. Their accelerating rotorod performance was very poor (Fig. 5C; $p = 0.0002$ vs. sham, $p < 0.002$ vs. 2.0- and 2.5-mm-impacted mice).

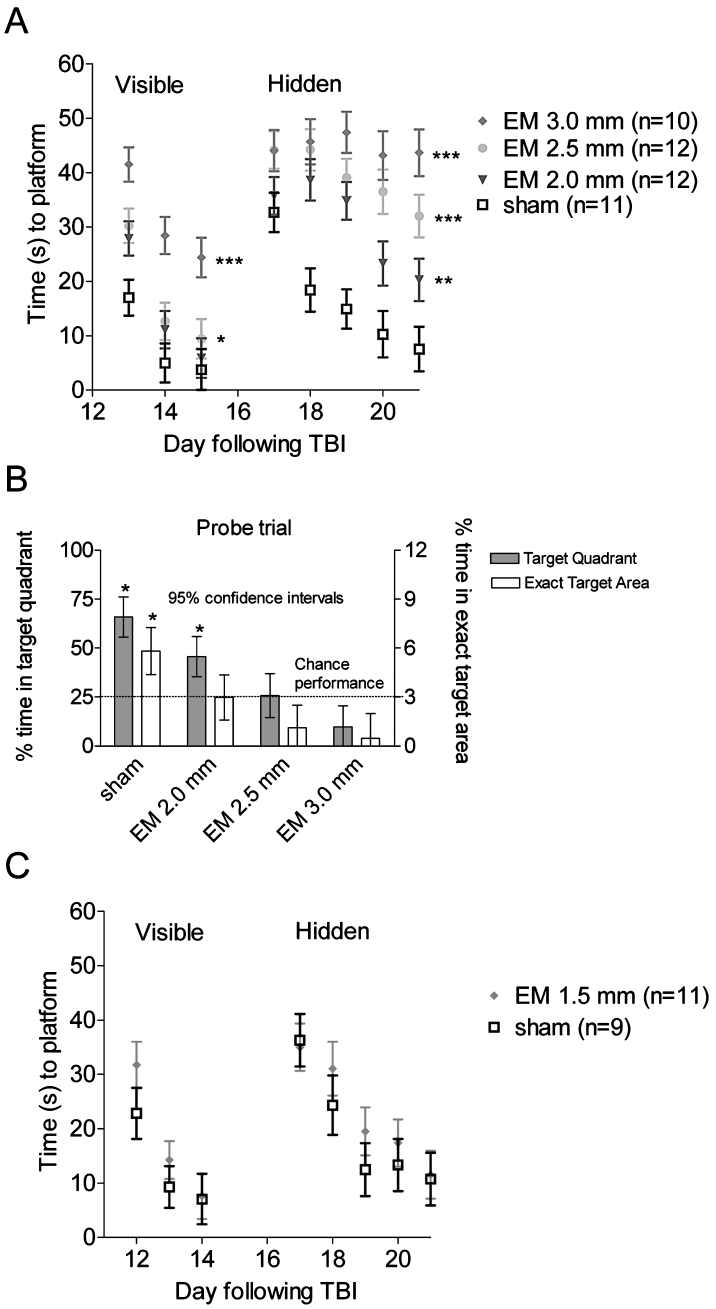

FIG. 4. Behavioral characterization of mice injured using the EM device in the Morris water maze. (**A**) Time to reach the platform as a function of day following experimental TBI. During visible platform testing, two of 12 mice subjected to 3.0-mm impacts failed to reliably swim to the platform and were disqualified from further water maze testing. No mice in the sham, 2.0-mm, or 2.5-mm impact groups were disqualified. Data shown represent mean and standard errors from the remaining, non-disqualified mice. During hidden platform testing, thre was a clear gradation in performance, with more severely injured animals performing worse. (***$p = 0.0002$, **$p = 0.006$, *$p = 0.039$, repeated-measures ANOVA followed by Tukey HSD post-hoc test for comparisons vs. sham). (**B**) Water maze probe testing; the platform was removed after the last day of hidden platform testing and mice were placed in the pool for a single, 30-sec trial. Sham mice spent considerably more time in the target quadrant and exact area where the platform had been than would have been expected by chance. Mice subjected to TBI had impaired performance, again in a graded fashion depending on the severity of injury (*95% confidence interval did not overlap with the performance expected by chance.) (**C**) In a separate experiment, mice subjected to a 1.5-mm impact did not show significant water maze performance deficits compared with concurrently tested, sham-injured mice.

These mice were also impaired in constant-velocity rotorod testing (Fig. 5B; $p = 0.0002$ vs. sham), again likely reflecting a deficit in procedural aspects of the testing or a severe motor learning deficit. In general, these mice were more lethargic and poorly groomed than mice with 2.0- and 2.5-mm injuries. Thus, there was a clear gradation in behavioral performance deficits as the depth of the injury increased.

We performed a separate, blinded experiment which demonstrated that 1.5-mm-impacted, wild-type, B6SJLF1 mice showed no statistically significant impairments in water maze performance compared with concurrently tested, sham-injured mice (Fig. 4C). A separate set of 2.5-mm-impacted mice was also tested concurrently and showed deficits consistent with those shown in the previous experiment (not shown).

To address sources of variability, we next asked whether male and female mice respond differently in this model of experimental TBI; the experiment was designed so that each group of mice contained equal numbers of males and females. In terms of hidden platform water maze performance, there was no overall effect of gender ($p = 0.38$), no interaction between injury severity and gender ($p = 0.29$), and a non-significant trend towards improved performance early in hidden platform testing which then equalized later in the testing ($p = 0.09$ for the interaction between day of testing and gender). Similarly, there were no effects of gender on cued or probe performance. In terms of rotorod performance, there was a trend towards improved performance of male mice in the accelerating phase which did not reach statistical significance ($p = 0.06$). There were no detectible interactions between gender and injury group ($p = 0.26$) or day of testing ($p = 0.48$). Thus we conclude that in this set of experiments, there were no major effects of gender and that this model of experimental TBI should be appropriate for testing mixed gender groups of mice. This is analogous to histological results reported previously (Hall et al., 2005).

In order to assess inter-operator reliability, two investigators each performed injuries on six mice at each level of injury severity. Mice were matched for age and sex between the two investigators. The two operators agreed on the design of the experiment and experimental details, but did not directly observe or critique each other's performance of the TBIs or sham injuries. All water maze testing was performed by a single investigator (D.L.B.), and all rotorod testing was performed by a single investigator (C.Y.). For hidden platform water maze testing, there was a significant difference between mice injured by the two investigators ($p = 0.0001$) and an interaction between investigator and injury severity ($p = 0.05$). Likewise, for visible platform water maze testing, there was a significant effect of investigator ($p = 0.003$) and an interaction between investigator and injury severity ($p = 0.01$). In both visible and hidden platform testing, the behavioral performance was indistinguishable for sham, and 2.0-mm and 2.5-mm impacts produced by the

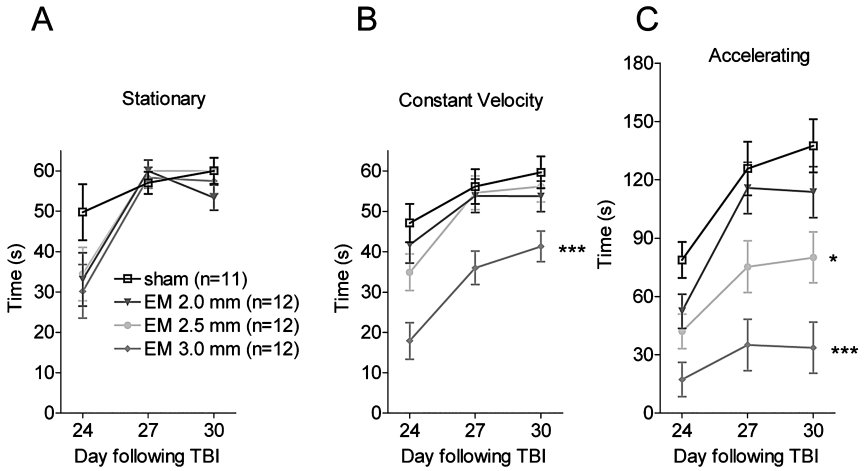

FIG. 5. Rotorod performance of mice injured using the EM device. Each mouse was tested on three separate days with one 60-sec stationary rod trial, two 60-sec constant velocity trials, and two 3-min accelerating trials. Data shown represent means and standard errors. All mice were included, even those disqualified from water maze testing. (**A**) Stationary rod performance. All mice performed well, even those subjected to the most severe injuries. (**B**) Constant velocity performance. Mice subjected to 3.0-mm impacts had impaired abilities to stay on the rod (***$p = 0.0002$ vs. sham) whereas milder injuries did not disrupt this ability. (**C**) Accelerating rod performance. There was a gradation of impairment with more severely injured animals performing worse (*$p = 0.016$, ***$p = 0.0002$ vs. sham).

two investigators. At 3.0 mm, there was a significant difference between investigators. There was no effect of investigator on rotorod performance ($p = 0.96$), nor was there an interaction between investigator and injury group ($p = 0.24$). Thus we conclude that reliability was good for 2.0- and 2.5-mm injuries but not for 3.0-mm injuries.

Sample Size Calculations Using Monte-Carlo Random Resampling

An important issue in the design of efficient preclinical treatment trials is sample size; in the design of preclinical treatment trials using rare and/or expensive transgenic mice, minimizing the sample size would be advantageous. To resolve a theoretical therapeutic effect on hidden platform performance of approximately the same magnitude as the difference between 3.0- and 2.5-mm impacts, our results suggest that 12 mice per group are appropriate, as our *p*-value was 0.038. A larger effect, similar to the difference between 2.0- and 3.0-mm impacts, however, could likely be resolved with fewer than 12 mice per group, as our *p*-value was 0.005. We therefore used Monte-Carlo random resampling followed by repeated-measures ANOVA to determine the sample size needed to obtain an 80% likelihood of detecting a statistically significant difference between two groups of mice with the properties of our 2.0- and 3.0-mm-injured animals. The advantages of this Monte-Carlo method are that it does not require any assumptions about the distribution of the data, and it can be used with data arising from measurements that are not independent of each other (such as repeated measurements of the same mice over time). These calculations indicated that, using the EM CCI device and this behavioral testing protocol, approximately seven to eight mice per group would be needed (Fig. 6).

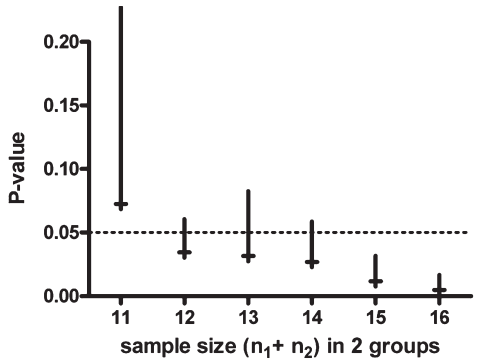

FIG. 6. Statistical power to distinguish between two injury severities in terms of hidden platform water maze performance. Monte-Carlo simulations were used based on original data sets from the 22 mice in the 2.0-mm and 3.0-mm impact groups. 150 random subsamples of these 22 mice were reanalyzed using repeated-measures ANOVA. For this analysis, the total number of mice in the random subsamples is plotted on the *x*-axis. The median and 80% confidence interval of the resulting *p*-values are plotted on the *y*-axis. This analysis indicates that, with 15 or greater total mice in the two groups, we would expect at least an 80% likelihood of detecting a difference between groups with a *p*-value of <0.05.

Effects of Impact Velocity on Injury Severity

A final issue that we addressed in this study was the effect of impact velocity on injury severity. We tested 3.0-mm impacts at 5.2 and at 3.6 m/sec (Fig. 7). There were no significant differences in the extent of spared tissue ($p = 0.98$ for hippocampus, $p = 0.36$ for cortex). Likewise, behavioral impairments were indistinguishable in water maze performance ($p = 0.57$ for visible platform, $p = 0.94$ for hidden platform) and rotorod performance ($p = 0.62$ for constant rotation speed, $p = 0.26$ for accelerating) between the two injury velocities. As noted above, there were no differences in stoke overshoot produced by the EM CCI device when velocity was changed from 5.2 to 3.6 m/sec (Fig. 2). In contrast, we found that reducing the velocity to 2.5 m/sec in the pneumatic impactor resulted in minimal histological injury following a 1-mm impact (data not shown), whereas there was substantial injury produced by a 1-mm impact at 5.2 m/sec (Fig. 3). Thus stroke velocity may exert an effect on injury severity primarily via effects on overshoot.

DISCUSSION

In summary, we have developed a stereotaxic, electromagnetic CCI device along with refined surgical and behavioral testing techniques. The device is capable of producing a wide range of injury severities, as assessed histologically and behaviorally; there was a clear gradation in both acute behavioral deficits and histological injury in adult wild-type mice as the impact depth was increased from 1.0 to 3.0 mm. Overall ease of use was excellent.

Strengths of the combined surgical, EM-CCI and behavioral testing technique described here include (1) very low mortality, (2) reliable, unbiased, stereotaxically defined injury production, and (3) good inter-operator reliability for most injury severities. This led to a relatively small number of mice per group needed to detect a statistically significant effect on behavioral outcomes following experimental TBI. Direct comparison of this efficiency to other injury models has not been performed. Further standardization of these procedures may improve the numbers needed even further.

There are several limitations to the conclusions that can be drawn from this study. First, we did not system-

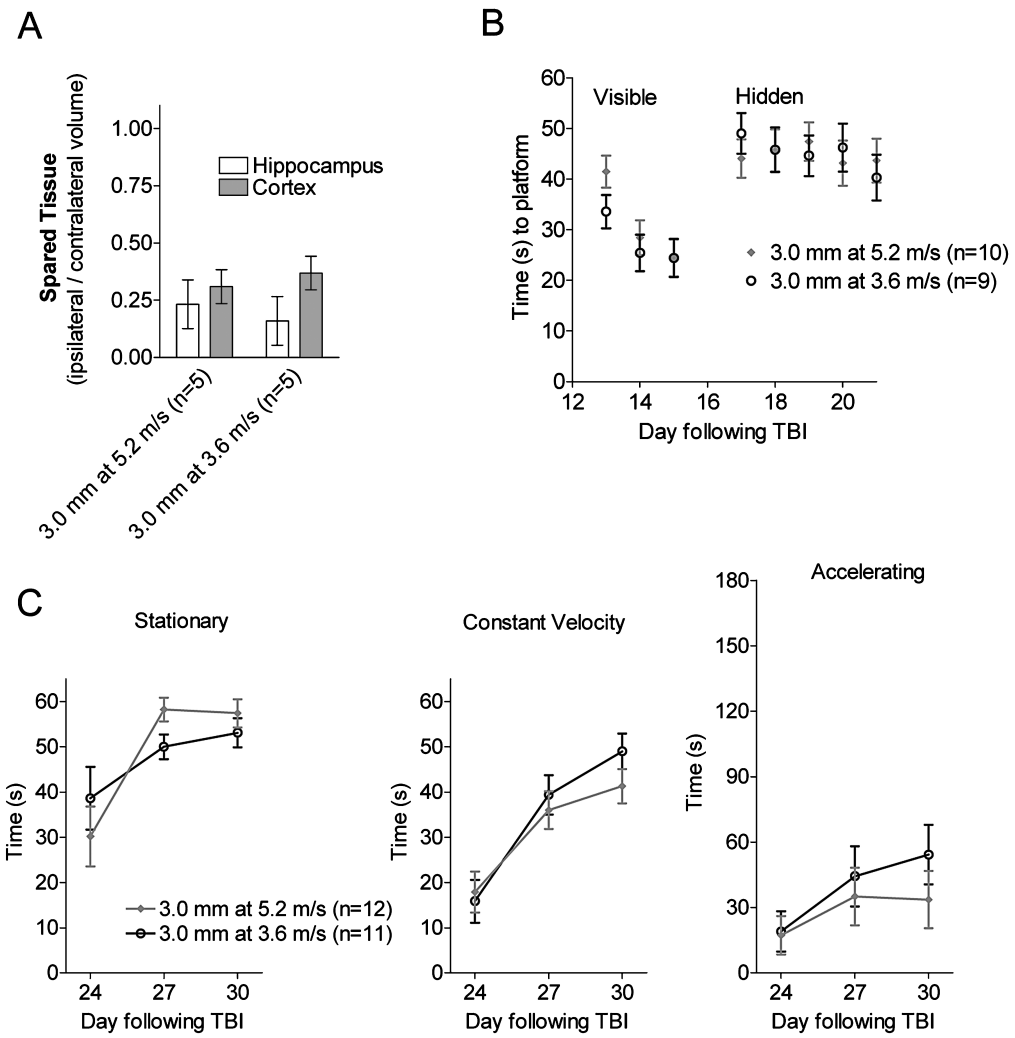

FIG. 7. Injury severity as a function of impact velocity. An additional group of WT mice were injured at 3.0-mm impact depth at a velocity of 3.6 m/sec and compared with 3.0-mm impats produced at a velocity of 5.2 m/sec. Data from the 5.2 m/sec groups is the same as that shown in Figures 3-5. (**A**) Fraction of spared tissue in hippocampus and cortex, assessed histologically, was not significantly different between groups. (**B**) Morris water maze performance. Two of 11 mice in the 3.0-mm at 3.6 m/sec group were disqualified from Morris water maze testing because of poor visible platform performance. The behavioral deficits in both visible and hidden platform performance were equally severe in both groups. (**C**) Rotored performance deficits were similar in the two groups.

atically test each of the individual variables in the preclinical TBI model, so we cannot definitively address the contribution of the CCI device itself, the isoflurane anesthesia, the touch detector, and maintenance of isothermia. However, the overall combination seems to yield a safe, consistent and convenient model for preclinical testing of TBI in mice. Second, we did not systematically test our injury model on other strains of mice, although our initial observations in a mouse model of Alzheimer's disease, PDAPP mice (Games et al., 1995) on a Swiss-Webster background suggest that histologically the injuries are very similar to those illustrated here for wild-type B6SJLF1 mice (data not shown). Third, issues of inter-operator reliability need to be investigated further; within our laboratory, inter-operator reliability was very good for 2.0- and 2.5-mm impacts, but not for 3.0-mm impacts. This may in part be due to post-procedural care of the animals. As noted above, 3.0-mm-impacted mice were lethargic and often lost weight following TBI. In the future, post-procedural animal care will need to be standardized for more severe injuries. An analogous issue is faced by multicenter clinical trials in human patients, where variability in outcomes and standards of care across centers has been raised as an important covariate

(Narayan et al., 2002). Finally, mice were sacrificed 1–2 months after injury, so long-term effects on behavioral performance were not assessed.

Our results differ in several important respects from those of Saatman et al. (2006) in which the authors reported a histological and behavioral comparison of 0.5- and 1.0-mm injuries produced using the AmScien pneumatic impact device. The previous report demonstrated behavioral abnormalities with even the mildest injuries (0.5-mm impact depth), whereas histologically comparable injuries in our study (1.5-mm impact depth) did not result in a detectible behavioral performance deficit. This may be due to differences in the behavioral testing procedures employed; the Saatman et al. group trained mice in the water maze before injury and then tested them for memory deficits 2 days following injury, whereas we performed all water maze, rotorod and conditioned fear testing starting 12 days after injury. These results are not incompatible, as it is likely that some behavioral performance deficits improve over time in the more mildly injured animals. Likewise, there were methodological differences in the way that the extent of injury in the cortex was determined in the two studies; lesion size in mm^3 was measured in Saatman et al., whereas we analyzed the fraction of spared tissue in the current study. Again, the results are not incompatible, as the same trend towards increasing lesion severity with increasing depths of injury was apparent in both studies.

The current model has not been tested outside of Washington University. Commercial development of the impactor system is in progress (MyNeurolab, St. Louis, MO) and will allow the next important step in reliability testing. As previous reports have shown considerable differences between groups in results of behavioral testing (Crabbe et al., 1999), the effects of these and other experimental brain injuries should be repeated in several laboratories to ensure that behavioral effects are reproducible.

We found that the impact depths required to produce substantial histologically defined lesions were higher than has been reported for injuries produced using pneumatic CCI devices (Smith et al., 1995; Saatman et al., 2006). This may be due to three factors: (1) the approximately 0.4-mm protrusion of the surface of the brain through the craniotomy due to mild compression of the skull by the cup head holders used instead of earbars; (2) the larger (0.6- vs. 0.3-mm) overshoot produced by the pneumatic device tested here; and (3) the use of a low-voltage electric circuit touch detector to set the zero point for the impact, as opposed to setting the zero point by eye. Other uncharacterized differences between techniques may also be important; further investigation will be required to obtain a full understanding of the relationship between mechanical characteristics of the impact and the severity of injury as measured using histological and behavioral techniques. This underscores the importance of pathophysiological readouts in the characterization and standardization of such devices.

The first and third factors listed above may also contribute to the explanation of why the set impact depth appears to cause a histological lesion that is less severe than would be expected based on the ~1-mm thickness of the mouse cortex. For example, it is likely that a 1.5-mm-depth impact does not appear to markedly injure the hippocampus because the 0.4-mm protrusion of the brain through the craniotomy and the early contact between the tip and brain surface afforded by the touch detector place the tip of the impactor approximately 1.5 mm from the edge of the hippocampus at the zero position. At 2-mm-impact depth, it is likely that the tip encroaches on the hippocampus, producing the gross anatomical distortion observed histologically. Furthermore, it should be emphasized that the brain may deform elastically during the impact; tissue beneath the impactor tip may move downwards or sideways transiently, and then return to its original position. Some of this tissue may be destroyed, but some may not. Thus, an impact at 1.5-mm depth is not necessarily equivalent to ablating a 1.5-mm-deep cylindrical volume of tissue.

Returning to the issue of overshoot, our measurement of the movement of the support structures during the impact strokes indicate that the overshoot arises largely from the deformation of these support structures: the stereotaxic arm for the EM device or metal support frame for the pneumatic device tested here. To reduce the overshoot of the EM device system, a more rigid stereotaxic arm could be employed. Similarly, a stiffer metal frame may reduce overshoot in the pneumatic device system. Although the pneumatic system we used has a more rigid support structure than the stereotaxic device, the pneumatic system provides much larger forces and involves more moving mass, which both contribute to overshoot. Other pneumatic devices produced by other manufacturers will need to be tested, as these may not be general characteristics of all such devices. The important point is that overshoot should be measured accurately for each individual electromagnetic or pneumatic device as part of its characterization.

Interestingly, we found no important differences in stroke overshoot and histological or behavioral outcomes produced by the EM CCI device when the velocity was changed from 5.2 to 3.6 m/sec. In light of our findings that overshoot was not highly dependent on velocity in this range, the current result with the EM impactor suggests that in fact, the depth of impact is the important factor in producing brain injury, and that the previously

reported effect of velocity (Fox et al., 1998) may have been due to velocity-dependent changes in overshoot. To confirm this, similar experiments should be performed with milder injuries and over a broader range of velocities. This issue may not have come to attention previously because measurements using the LVDT technique did not reveal as prominent an overshoot as we found using laser Doppler measurements. The laser Doppler has a much faster response (10,000-Hz specified bandwidth) than LVDTs (typically 200–300 Hz bandwidth). The greater bandwidth specifically enables the laser Doppler sensor to measure the sub-millisecond events typical of impacts. The laser Doppler sensor also measures the movement of the impactor tip directly, unlike the LVDT, which measures the movement of the back of the impactor shaft. In fact, the LVDT itself would be expected to move along with the frame during the impact stroke, making LVDT measurements of overshoot caused by frame movement largely unreliable, although they appear adequate for measurements of velocity.

Several interesting results arose from the behavioral testing performed here. First, it appeared that spatial learning performance was the most sensitive behavioral indicator of brain injury, as 2.0-mm-impacted mice showed deficits only in this domain. Second, with more severe injury, there were motor learning deficits that persisted into the subacute period. As there was not apparent injury to the cerebellum or brainstem in any of these mice (data not shown), these motor learning deficits may reflect the effects of the extensive white matter injury that accompanies the deeper impacts (Mac Donald et al., unpublished data). Third, we did not find a significant effect of gender in severity of injury in these experiments. It has been suggested that the apparent protective effect of female gender and/or female sex hormones may be more prominent in animal models of widely diffuse TBI than in focal injuries such as CCI with more rapid neurodegeneration (Hall et al., 2005a). Our results are consistent with this hypothesis. Fourth, we did not observe deficits in conditioned fear performance, even in the most severely injured mice. The ability to associate an aversive stimulus with environmental and sensory cues appears to be a robust one. As this task has been reported to be sensitive to both hippocampal and amygdala function (Crawley, 2000), it would be interesting to explore the effects of contusions directly targeting the amygdala on conditioned fear performance.

CONCLUSION

We have developed and characterized an electromagnetic, stereotaxically mounted CCI device for producing experimental TBI in mice. The device is reliable, easy to use, and capable of producing injuries that cause behavioral impairments and histologically defined lesions ranging from mild to severe. We hope that this device will aid in the development of reproducible, uniform mouse models of TBI. The importance of this work is underscored by the growing emphasis in TBI research on the use of transgenic and other types of genetically modified mice with manipulations of relevant human genes.

ACKNOWLEDGMENTS

P.V.B., C.C.K., and Washington University may receive income based on a license of related technology to MyNeuroLab. Support was provided by NIH (D.L.B.: NS049237; to D.M.H.: AG13956), Burroughs Wellcome (to D.L.B.), and myNeurolab (to P.V.B., via NIH SBIR grants R43 NS046825 and R44 NS46825).

REFERENCES

ABRAHAMSON, E.E., IKONOMOVIC, M.D., CIALLELLA, J.R., et al. (2006). Caspase inhibition therapy abolishes brain trauma-induced increases in Abeta peptide: implications for clinical outcome. Exp. Neurol. **197,** 437–450.

BAYIR, H., CLARK, R.S., and KOCHANEK, P.M. (2003). Promising strategies to minimize secondary brain injury after head trauma. Crit. Care Med. **31,** S112–S117.

BAYIR, H., KAGAN, V.E., BORISENKO, G.G., et al. (2005). Enhanced oxidative stress in iNOS-deficient mice after traumatic brain injury: support for a neuroprotective role of iNOS. J. Cereb. Blood Flow Metab. **25,** 673–684.

BAYLY, P.V., DIKRANIAN, K.T., BLACK, E.E., et al. (2006). Spatiotemporal evolution of apoptotic neurodegeneration following traumatic injury to the developing rat brain. Brain Res. **1107,** 70–81.

BERMPOHL, D., YOU, Z., KORSMEYER, S.J., MOSKOWITZ, M.A., and WHALEN, M.J. (2006). Traumatic brain injury in mice deficient in Bid: effects on histopathology and functional outcome. J. Cereb. Blood Flow Metab. **26,** 625–633.

BRODY, D.L., and HOLTZMAN, D.M. (2006). Morris water maze search strategy analysis in PDAPP mice before and after experimental traumatic brain injury. Exp. Neurol. **197,** 330–340.

BUKI, A., and POVLISHOCK, J.T. (2006). All roads lead to disconnection?—traumatic axonal injury revisited. Acta Neurochir. (Wien.) **148,** 181–193.

CHANG, E.F., WONG, R.J., VREMAN, H.J., et al. (2003). Heme oxygenase-2 protects against lipid peroxidation-mediated cell loss and impaired motor recovery after traumatic brain injury. J. Neurosci. **23,** 3689–3696.

CONTE, V., URYU, K., FUJIMOTO, S., et al. (2004). Vitamin E reduces amyloidosis and improves cognitive function

in Tg2576 mice following repetitive concussive brain injury. J. Neurochem. **90,** 758–764.

CRABBE, J.C., WAHLSTEN, D., and DUDEK, B.C. (1999). Genetics of mouse behavior: interactions with laboratory environment. Science **284,** 1670–1672.

CRAWLEY, J.N. (2000). *What's Wrong with My Mouse?* Wiley-Liss: New York.

DIXON, C.E., CLIFTON, G.L., LIGHTHALL, J.W., YAGHMAI, A.A., and HAYES, R.L. (1991). A controlled cortical impact model of traumatic brain injury in the rat. J. Neurosci. Methods **39,** 253–262.

DUHAIME, A.C., MARGULIES, S.S., DURHAM, S.R., et al. (2000). Maturation-dependent response of the piglet brain to scaled cortical impact. J. Neurosurg. **93,** 455–462.

FADEN, A.I., MOVSESYAN, V.A., KNOBLACH, S.M., AHMED, F., and CERNAK, I. (2005). Neuroprotective effects of novel small peptides *in vitro* and after brain injury. Neuropharmacology **49,** 410–424.

FOX, G.B., FAN, L., LEVASSEUR, R.A., and FADEN, A.I. (1998). Sustained sensory/motor and cognitive deficits with neuronal apoptosis following controlled cortical impact brain injury in the mouse. J. Neurotrauma **15,** 599–614.

FRANKLIN, K.B., and PAXINOS, G. (1997). *The Mouse Brain in Stereotaxic Coordinates*. Academic Press: London.

FUJIMOTO, S.T., LONGHI, L., SAATMAN, K.E., CONTE, V., STOCCHETTI, N., and McINTOSH, T.K. (2004). Motor and cognitive function evaluation following experimental traumatic brain injury. Neurosci. Biobehav. Rev. **28,** 365–378.

GAMES, D., ADAMS, D., ALESSANDRINI, R., et al. (1995). Alzheimer-type neuropathology in transgenic mice overexpressing V717F beta-amyloid precursor protein. Nature **373,** 523–527.

HALL, E.D., GIBSON, T.R., and PAVEL, K.M. (2005a). Lack of a gender difference in post-traumatic neurodegeneration in the mouse controlled cortical impact injury model. J. Neurotrauma **22,** 669–679.

HALL, E.D., SULLIVAN, P.G., GIBSON, T.R., PAVEL, K.M., THOMPSON, B.M., and SCHEFF, S.W. (2005b). Spatial and temporal characteristics of neurodegeneration after controlled cortical impact in mice: more than a focal brain injury. J. Neurotrauma **22,** 252–265.

HARTMAN, R.E., LAURER, H., LONGHI, L., et al. (2002). Apolipoprotein E4 influences amyloid deposition but not cell loss after traumatic brain injury in a mouse model of Alzheimer's disease. J. Neurosci. **22,** 10083–10087.

HLATKY, R., LUI, H., CHERIAN, L., et al. (2003). The role of endothelial nitric oxide synthase in the cerebral hemodynamics after controlled cortical impact injury in mice. J. Neurotrauma **20,** 995–1006.

HOLTZMAN, D.M., BALES, K.R., TENKOVA, T., et al. (2000). Apolipoprotein E isoform-dependent amyloid deposition and neuritic degeneration in a mouse model of Alzheimer's disease. Proc. Natl. Acad. Sci. USA **97,** 2892–2897.

HOWARD, V., and REED, M.G. (2005). Unbiased Stereology: Three-Dimensional Measurement in Microscopy, 2nd ed. Oxon: Abingdon, UK.

JELLINGER, K.A. (2004). Head injury and dementia. Curr. Opin. Neurol. **17,** 719–723.

KHUCHUA, Z., WOZNIAK, D.F., BARDGETT, M.E., et al. (2003). Deletion of the N-terminus of murine map2 by gene targeting disrupts hippocampal CA1 neuron architecture and alters contextual memory. Neuroscience **119,** 101–111.

KLEINDIENST, A., McGINN, M.J., HARVEY, H.B., COLELLO, R.J., HAMM, R.J., and BULLOCK, M.R. (2005). Enhanced hippocampal neurogenesis by intraventricular S100B infusion is associated with improved cognitive recovery after traumatic brain injury. J. Neurotrauma **22,** 645–655.

KOCHANEK, P.M., VAGNI, V.A., JANESKO, K.L., et al. (2006). Adenosine A1 receptor knockout mice develop lethal status epilepticus after experimental traumatic brain injury. J. Cereb. Blood Flow Metab. **26,** 565–575.

LAURER, H.L., and McINTOSH, T.K. (1999). Experimental models of brain trauma. Curr. Opin. Neurol. **12,** 715–721.

LENZLINGER, P.M., SHIMIZU, S., MARKLUND, N., et al. (2005). Delayed inhibition of Nogo-A does not alter injury-induced axonal sprouting but enhances recovery of cognitive function following experimental traumatic brain injury in rats. Neuroscience **134,** 1047–1056.

LIGHTHALL, J.W., DIXON, C.E., and ANDERSON, T.E. (1989). Experimental models of brain injury. J. Neurotrauma **6,** 83–97.

LONGHI, L., SAATMAN, K.E., RAGHUPATHI, R., et al. (2001). A review and rationale for the use of genetically engineered animals in the study of traumatic brain injury. J. Cereb. Blood Flow Metab. **21,** 1241–1258.

MAEGELE, M., LIPPERT-GRUENER, M., ESTER-BODE, T., et al. (2005). Reversal of neuromotor and cognitive dysfunction in an enriched environment combined with multimodal early onset stimulation after traumatic brain injury in rats. J. Neurotrauma **22,** 772–782.

MARKLUND, N., FULP, C.T., SHIMIZU, S., et al. (2006). Selective temporal and regional alterations of Nogo-A and small proline-rich repeat protein 1A (SPRR1A) but not Nogo-66 receptor (NgR) occur following traumatic brain injury in the rat. Exp. Neurol. **197,** 70–83.

MARMAROU, C.R., and POVLISHOCK, J.T. (2006). Administration of the immunophilin ligand FK506 differentially attenuates neurofilament compaction and impaired axonal transport in injured axons following diffuse traumatic brain injury. Exp. Neurol. **197,** 353–362.

MAXWELL, W.L., WATSON, A., QUEEN, R., et al. (2005). Slow, medium, or fast re-warming following post-traumatic hypothermia therapy? An ultrastructural perspective. J. Neurotrauma **22,** 873–884.

MEANEY, D.F., ROSS, D.T., WINKELSTEIN, B.A., et al. (1994). Modification of the cortical impact model to produce axonal injury in the rat cerebral cortex. J. Neurotrauma **11,** 599–612.

MORALES, D.M., MARKLUND, N., LEBOLD, D., et al. (2005). Experimental models of traumatic brain injury: Do we really need to build a better mousetrap? Neuroscience **136,** 971–989.

MURAI, H., PIERCE, J.E., RAGHUPATHI, R., et al. (1998).

Twofold overexpression of human beta-amyloid precursor proteins in transgenic mice does not affect the neuromotor, cognitive, or neurodegenerative sequelae following experimental brain injury. J. Comp. Neurol. **392,** 428–438.

NARAYAN, R.K., MICHEL, M.E., ANSELL, B., et al. (2002). Clinical trials in head injury. J. Neurotrauma **19,** 503–557.

PINEDA, J.A., WANG, K.K., and HAYES, R.L. (2004). Biomarkers of proteolytic damage following traumatic brain injury. Brain Pathol. **14,** 202–209.

PRINS, M.L., FUJIMA, L.S., and HOVDA, D.A. (2005). Age-dependent reduction of cortical contusion volume by ketones after traumatic brain injury. J. Neurosci. Res. **82,** 413–420.

SAATMAN, K.E., FEEKO, K.J., PAPE, R.L., and RAGHUPATHI, R. (2006). Differential behavioral and histopathological responses to graded cortical impact injury in mice. J. Neurotrauma **23,** 1241–1253.

SABO, T., LOMNITSKI, L., NYSKA, A., et al. (2000). Susceptibility of transgenic mice expressing human apolipoprotein E to closed head injury: the allele E3 is neuroprotective whereas E4 increases fatalities. Neuroscience **101,** 879–884.

SHOHAMI, E., NOVIKOV, M., and BASS, R. (1995). Long-term effect of HU-211, a novel non-competitive NMDA antagonist, on motor and memory functions after closed head injury in the rat. Brain Res. **674,** 55–62.

SMITH, D.H., SOARES, H.D., PIERCE, J.S., et al. (1995). A model of parasagittal controlled cortical impact in the mouse: cognitive and histopathologic effects. J. Neurotrauma **12,** 169–178.

SMITH, D.H., NAKAMURA, M., McINTOSH, T.K., et al. (1998). Brain trauma induces massive hippocampal neuron death linked to a surge in beta-amyloid levels in mice overexpressing mutant amyloid precursor protein. Am. J. Pathol. **153,** 1005–1010.

SULLIVAN, P.M., MEZDOUR, H., ARATANI, Y., et al. (1997). Targeted replacement of the mouse apolipoprotein E gene with the common human APOE3 allele enhances diet-induced hypercholesterolemia and atherosclerosis. J. Biol. Chem. **272,** 17972–17980.

SUN, Y., WU, S., BU, G., et al. (1998). Glial fibrillary acidic protein–apolipoprotein E (apoE) transgenic mice: astrocyte-specific expression and differing biological effects of astrocyte-secreted apoE3 and apoE4 lipoproteins. J. Neurosci. **18,** 3261–3272.

TEASDALE, G.M., MURRAY, G.D., and NICOLL, J.A. (2005). The association between APOE epsilon4, age and outcome after head injury: a prospective cohort study. Brain **128,** 2556–2561.

THOMPSON, H.J., LIFSHITZ, J., MARKLUND, N., et al. (2005). Lateral fluid percussion brain injury: a 15–year review and evaluation. J. Neurotrauma **22,** 42–75.

THURMAN, D.J., ALVERSON, C., DUNN, K.A., GUERRERO, J., and SNIEZEK, J.E. (1999). Traumatic brain injury in the United States: a public health perspective. J. Head Trauma Rehabil. **14,** 602–615.

TRUETTNER, J.S., SUZUKI, T., and DIETRICH, W.D. (2005). The effect of therapeutic hypothermia on the expression of inflammatory response genes following moderate traumatic brain injury in the rat. Brain Res. Mol. Brain Res. **138,** 124–134.

URYU, K., LAURER, H., McINTOSH, T., et al. (2002). Repetitive mild brain trauma accelerates A_{beta} deposition, lipid peroxidation, and cognitive impairment in a transgenic mouse model of Alzheimer amyloidosis. J. Neurosci. **22,** 446–454.

XU, P.T., SCHMECHEL, D., ROTHROCK-CHRISTIAN, T., et al. (1996). Human apolipoprotein E2, E3, and E4 isoform-specific transgenic mice: human-like pattern of glial and neuronal immunoreactivity in central nervous system not observed in wild-type mice. Neurobiol. Dis. **3,** 229–245.

Address reprint requests to:
David L. Brody, M.D.
Box 8111
660 S. Euclid Avenue
St. Louis, MO 63110

E-mail: brodyd@neuro.wustl.edu